6-13-2009

Atmospheric Condensed-Phase Reactions of Glyoxal with Methylamine

David O. De Haan
University of San Diego, ddehaan@sandiego.edu

Margaret A. Tolbert
University of Colorado Boulder

Jose L. Jimenez
University of Colorado Boulder

Digital USD Citation

De Haan, David O.; Tolbert, Margaret A.; and Jimenez, Jose L., "Atmospheric Condensed-Phase Reactions of Glyoxal with Methylamine" (2009). *Chemistry and Biochemistry: Faculty Scholarship*. 17.
https://digital.sandiego.edu/chemistry_facpub/17

Atmospheric Condensed-Phase Reactions of Glyoxal with Methylamine

Abstract

[1] Glyoxal reacts with methylamine in drying cloud droplet/aerosol surrogates to form high molecular mass oligomers along with smaller amounts of *1,3*-dimethylimidazole and light-absorbing compounds. The patterns observed by high-resolution time-of-flight aerosol mass spectrometry indicate that oligomers form from repeated imine units. The reactions are 1st order in each reactant: rate-limiting imine formation is followed by rapid dimer and oligomer formation. While excess methylamine evaporates from the droplet, half the glyoxal does not, due to self-oligomerization reactions that occur in the absence of methylamine. Glyoxal irreversibly traps volatile amine compounds in the aerosol phase, converting them into oligomers. This is the first reported mechanism for the formation of stable secondary organic aerosol (SOA) material from methylamine, a substance with only one carbon, and could produce as much as 11 Tg SOA yr^{-1} globally if glyoxal reacts exclusively by this pathway.

Keywords

Glyoxal, Cloud Processing, Secondary Organic Aerosol

GEOPHYSICAL RESEARCH LETTERS, VOL. 36, L11819, doi:10.1029/2009GL037441, 2009

Atmospheric condensed-phase reactions of glyoxal with methylamine

David O. De Haan,[1,2] Margaret A. Tolbert,[2] and Jose L. Jimenez[2]

Received 23 January 2009; revised 20 March 2009; accepted 11 May 2009; published 13 June 2009.

[1] Glyoxal reacts with methylamine in drying cloud droplet/aerosol surrogates to form high molecular mass oligomers along with smaller amounts of *1,3*-dimethylimidazole and light-absorbing compounds. The patterns observed by high-resolution time-of-flight aerosol mass spectrometry indicate that oligomers form from repeated imine units. The reactions are 1st order in each reactant: rate-limiting imine formation is followed by rapid dimer and oligomer formation. While excess methylamine evaporates from the droplet, half the glyoxal does not, due to self-oligomerization reactions that occur in the absence of methylamine. Glyoxal irreversibly traps volatile amine compounds in the aerosol phase, converting them into oligomers. This is the first reported mechanism for the formation of stable secondary organic aerosol (SOA) material from methylamine, a substance with only one carbon, and could produce as much as 11 Tg SOA yr^{-1} globally if glyoxal reacts exclusively by this pathway. **Citation:** De Haan, D. O., M. A. Tolbert, and J. L. Jimenez (2009), Atmospheric condensed-phase reactions of glyoxal with methylamine, *Geophys. Res. Lett.*, *36*, L11819, doi:10.1029/2009GL037441.

1. Introduction

[2] Laboratory simulations [*Kalberer et al.*, 2004; *Nozière et al.*, 2007; *Tolocka et al.*, 2004] and field measurements [*Baltensperger et al.*, 2005; *Denkenberger et al.*, 2007; *Kalberer et al.*, 2006] have suggested that complex, light-absorbing oligomers with masses near several hundred amu are a major water-soluble component of atmospheric secondary organic aerosol (SOA). Aldehydes are likely involved in their formation, since they form oligomers in aqueous-phase reactions accelerated by drying [*Kalberer et al.*, 2004] or catalyzed by amino acids or ammonium salts [*Nozière et al.*, 2007]. *Denkenberger et al.* [2007] found that all oligomer-containing particles sampled in Riverside, CA exhibited strong aerosol time-of-flight mass spectrometer signals of both amines and oxalic acid, an aqueous-phase oxidation product of glyoxal [*Carlton et al.*, 2007].

[3] Single-component chamber photooxidation experiments performed in the absence of glyoxal have demonstrated that methylamine does not generate significant aerosol mass [*Malloy et al.*, 2008; *Murphy et al.*, 2007; *Silva et al.*, 2008]. However, as shown in this work, methylamine forms oligomerized SOA during simulated cloud droplet/aerosol drying in the presence of glyoxal. Both compounds are commonly present in clouds and aerosol [*Igawa et al.*, 1989; *Zhang and Anastasio*, 2003]. It has recently been shown that reactions between glyoxal and amino acids in evaporating droplets and aerosol surrogates form stable imidazoles along with light-absorbing compounds [*De Haan et al.*, 2009]. C–N bond formation was also observed in aqueous-phase reactions of glyoxal with ammonium sulfate aerosol, and was attributed to imidazole formation [*Galloway et al.*, 2008]. In this work we characterize reactions between glyoxal and methylamine using electrospray ionization mass spectrometry (ESI-MS), nuclear magnetic resonance (NMR) spectroscopy, and both quadrupole and high-resolution time-of-flight aerosol MS (Q-AMS and HR-ToF-AMS). We analyze the concentration dependence of the reaction and the partitioning of excess reactants when aqueous droplets are exposed to decreasing relative humidity.

2. Experimental Methods

[4] Glyoxal trimer dihydrate and a 40% w/w aqueous solution of methylamine (Sigma-Aldrich) were used without further purification. Since aqueous phase reactions of glyoxal are greatly accelerated by drying [*Loeffler et al.*, 2006], all experiments included a drying step performed at room temperature, either in air for bulk experiments or in humidified nitrogen for simulated cloud droplet evaporation experiments. Product formation in bulk-phase reactions was studied by mixing 150 μL aliquots of 1 M glyoxal and methylamine solutions in glass vials and allowing the solutions to dry in air at 295 K. The resulting deep brown residue was characterized by re-dissolving in D_2O or water at 1 mg/mL and analyzing by ^{1}H-NMR (400 MHz), ESI-MS (Thermo-Finnigan LCQ Advantage, ESI nozzle voltage = +4.3 kV, injection rate 2.5 μL/min, medical N_2 sheath gas flow = 25, capillary temperature = 250°C), and HR-ToF-AMS (Aerodyne Research, vaporization temp. of 600 °C, electron ionization (EI) at 70 eV) [*DeCarlo et al.*, 2006].

[5] Concentration dependence was studied in drying aerosol experiments by ultrasonically nebulizing aqueous solutions containing <0.1 wt% total organics, which is less than an order of magnitude above measured levels in anthropogenically-influenced clouds [*Decesari et al.*, 2005]. Droplets with wet diameters near 4 μm were neutralized (NRD model P-2021-1000) and sent via N_2 flow and copper tubing into a 300 L Teflon chamber (New Star Environmental, LLC) containing nitrogen humidified to >70% relative humidity (RH). RH was monitored at the chamber outlet (Vaisala HMT337). After 10–20 minutes of fill time, the particles in the chamber were sampled via black conductive (TSI) or copper tubing by scanning mobility particle sizing (SMPS, TSI Inc. models 3080, 3081, 3010),

---

[1] Department of Chemistry and Biochemistry, University of San Diego, San Diego, California, USA.

[2] Department of Chemistry and Biochemistry and Cooperative Institute for Research in Environmental Sciences, University of Colorado, Boulder, Colorado, USA.

0094-8276/09/2009GL037441

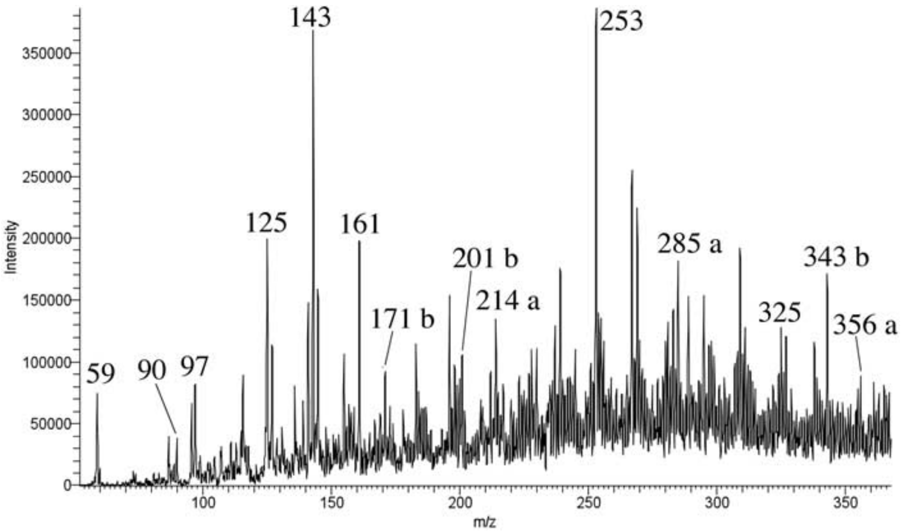

Figure 1. Positive mode ESI-MS spectrum of the products of bulk phase reaction of glyoxal with methylamine, re-dissolving in water at 1 mg/mL. a and b are labels for the oligomer series shown in Figure 2.

Q-AMS (Aerodyne Research, conditions as above) [*Canagaratna et al.*, 2007], and/or HR-ToF-AMS (*W* mode).

3. Results and Discussion

[6] The ESI-MS spectrum of the products of the bulk-phase reaction of glyoxal and methylamine are shown in Figure 1. Nucleophilic attack by the amine group on the glyoxal aldehyde group produces an imine in a drying aqueous droplet (Figure 2). A protonated, hydrated imine could be responsible for the peak detected at *m/z* 90 by ESI-MS (Figure 1). However, peaks assigned to 2nd generation imine reaction products are larger: a peak at *m/z* 97 is consistent with *1,3*-dimethylimidazole, and a prominent *mz = 18* series (Δ*m/z* 125, 143, and 161) is likely due to protonated imine dimers incorporating varying amounts of

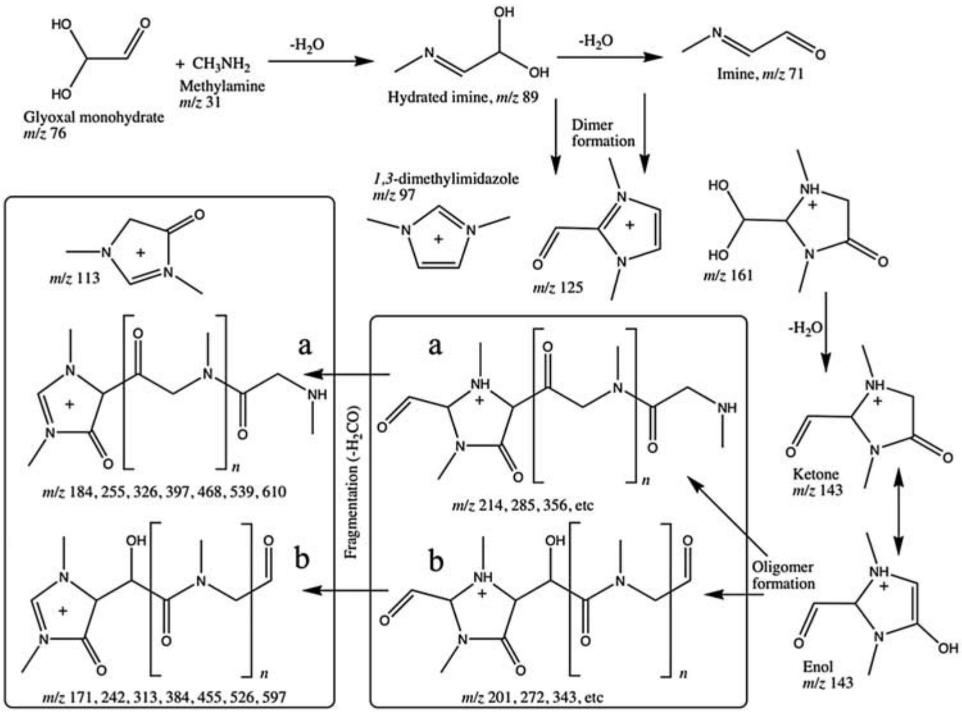

Figure 2. Potential structures of imine dimers and oligomers formed in the reactions of glyoxal with methylamine during cloud droplet evaporation. Aldehyde groups, while completely hydrated in aqueous-phase NMR measurements (and thus not observed in Figure S1 of the auxiliary material), are only partially hydrated in ESI-MS and unhydrated in AMS measurements due to solvent evaporation in the inlet regions. a and b are the oligomer series marked in Figures 1 and 3. Left box: fragment ions observed by AMS. Right box: oligomer molecules observed mainly by ESI-MS.

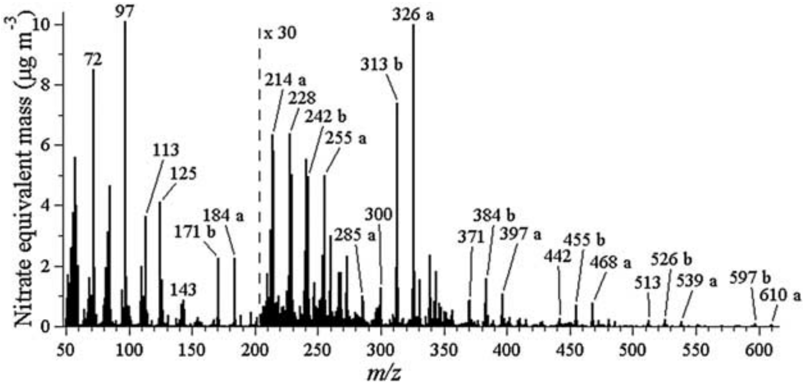

Figure 3. HR-ToF-AMS stick spectrum of aerosol produced from solution containing 8.8 mM glyoxal and 16.8 mM methylamine, dried at 90%RH in a chamber for 10 min. a and b are labels for the oligomer series shown in Figure 2. The peak height at *m/z* 597 is 11 times higher than the background measured when sampling non-oligomer-forming systems.

water. A series of oligomeric groups with Δ*m/z* of 12, 13 and 14, peaking at *m/z* 253, and extending well beyond *m/z* 800 as a continuous elevated baseline, are also detected by ESI-MS. None of these groups or patterns were observed in the absence of methylamine [*Hastings et al.*, 2005], and the magnitude of the baseline signal was ten times lower than in Figure 1. These patterns, as will be shown below, are consistent with the formation of imine oligomers.

[7] In order to probe these reactions under more atmospherically relevant conditions, aqueous aerosol drying was simulated in chamber experiments. In 10 min at 90% RH, droplets containing 8.8 mM glyoxal and 17 mM methylamine lost >99.99% of their volume due to water loss, and the resulting aerosol particles contained significant amounts of oligomerized products, as seen by AMS (Figure 3). Decomposition during AMS aerosol evaporation adds to strong EI fragmentation at 70 *eV* (their combined effect we will refer to as "fragmentation" below), while unfragmented parent molecules (as H+ adducts) are detected by ESI-MS. While ESI-MS spectra are typically simpler than AMS spectra, in this case the complex oligomeric pattern detected with ESI-MS (Figure 1), resolves in the HR-ToF-AMS into superimposed Δ*m/z* 13 and Δ*m/z* 71 patterns (Figure 3), indicating that many oligomers decompose into the same "building-block" fragments. These patterns, analyzed at high resolution for exact mass information, suggest that oligomers are rapidly formed by repeated additions of the imine ($CH_3N{=}CHCHO$, *m/z* 71). Potential product structures consistent with exact mass and NMR data (Figure S1 of the auxiliary material) are shown in Figure 2.[1] A peak consistent with the protonated imine is observed by AMS at *m/z* 72. The ESI-MS peaks assigned to imine dimers are again visible by AMS at *m/z* 125 and 143, but peaks assigned to hydrated species (*m/z 90, 161)* are negligible due to water loss during fragmentation. The prominent peak at *m/z* 97 is consistent with *1,3*-dimethylimidazole. See Figures S2–S4 for control runs.

[8] The proposed imine dimer structures with aldehyde groups have enol tautomers that can undergo aldol condensation with glyoxal or imine molecules, as shown in Figure 2. The *m/z* 214, 285, 356 "a" series could result from the repeated addition of imine molecules to a *m/z* 143 dimer. The addition of glyoxal by aldol condensation, followed by imine addition, could produce the *m/z* 201, 272, 343 "b" series. Most of these peaks are visible in the ESI mass spectrum (Figure 1). However, except for *m/z* 214, these peaks are not prominent in the AMS spectrum (Figure 3) likely because of H_2CO loss (Δ*m/z* -30) during fragmentation. Loss of H_2CO can produce the corresponding fragment series *m/z* 171, 242, 313, 384, 455, 546, 597 ("b") and 184, 255, 326, 297, 468, 539, 610 ("a") shown in the left box in Figure 2. These fragment peaks dominate the AMS spectrum, but with the exception of *m/z* 171, are not prominently observed by ESI-MS, as expected. A third Δ*m/z* 71 series is observed at 229, 300, 371, 442, and 513, likely due to hydrolysis and loss of a methylamine unit (Δ*m/z* −13) from the series starting at *m/z* 171. The base of all of these fragment ion series appears to be the dimer fragment observed in Figure 3 at *m/z* 113 ($C_5H_9N_2O$), formed either by H_2CO loss from a *m/z* 143 imine dimer or by oligomer fragmentation.

3.1. Concentration Dependence

[9] The concentration dependence of glyoxal + methylamine reactions was studied by independently varying the concentrations of each reactant in aqueous droplets, evaporating the droplets at RH > 70%, and analyzing the resulting aerosol by Q-AMS. In the first set of experiments, glyoxal concentrations were varied from 0 to 8.8 mM while [methylamine] = 16.8 mM. Fifteen different product ions were analyzed (Figure S5) and were found to vary as a function of $[\text{glyoxal}]^{1.0 \pm 0.2}$, indicating that the reaction is 1st order with respect to glyoxal, consistent with the reaction of glyoxal with ammonium salts under similar conditions (pH < 6 and $[NH_4^+] < 2$ M) [*Nozière et al.*, 2009]. In a second experiment, [glyoxal] = 8.8 mM while methylamine concentrations were varied between 0.35 and 9.3 mM. Four product ions (that were not produced by glyoxal in the absence of methylamine) varied proportionally to $[\text{methylamine}]^{0.8 \pm 0.3}$. The total reaction order is thus 1.8 ± 0.4 (2nd order overall), the same as that determined for glyoxal + amino acid reactions by a similar analysis and by ^{1}H-NMR kinetics [*De Haan et al.*, 2009]. The formation of oligomers and imidazole derivatives (that contain two or more molecules of each reactant) in reactions that are 1st

---

[1] Auxiliary materials are available in the HTML. doi:10.1029/2009GL037441.

order in each reactant suggests that imine formation is the rate-limiting step. The imine appears to be an intermediate in the production of oligomers, which is likely the reason it is not detected in longer, bulk-phase experiments.

3.2. Reactant Volatilization

[10] The glyoxal + methylamine experiments just described also provide information about volatilization of the reactants. In experiments where droplet glyoxal concentrations are very low relative to methylamine, if the excess methylamine evaporates, very little material will be left behind as aerosol when water evaporates from the droplet. This is exactly what is observed in three SMPS experiments (Figure S6). When the concentration of glyoxal is low, minimal aerosol is produced; furthermore, Q-AMS imidazole product peaks at *m/z* 97, 42, and 15 disappear. When glyoxal is added in, it reacts with an equivalent amount of methylamine and aerosol volumes are seen to increase sharply, demonstrating that glyoxal traps methylamine in the aerosol phase via the reactions described above.

[11] The behavior of glyoxal is fundamentally different. If all excess glyoxal partitioned to the gas phase upon droplet evaporation, very little aerosol material would be observed when methylamine concentrations are low. Instead, aerosol volumes remain high when methylamine concentrations are low. When methylamine is added in, glyoxal peaks decline and imidazole and imine peaks reappear in the aerosol mass spectrum (Figures S2, S7, and 3), but aerosol volumes increase by only 48% (Figure S6, circles). This nearly matches the theoretical volume increase of 47% if the same fraction of glyoxal remained in the aerosol phase but reacted with methylamine instead of itself (assuming that both reactions produce oligomers of the same density). Comparing these SMPS size distributions with that of NaCl aerosol generated under the same conditions indicates that about half of the glyoxal volatilizes from drying droplets initially containing 8.8 mM glyoxal in 1 h at RH > 70%, whether or not methylamine is present. This is consistent with recent observations of glyoxal volatilization from aqueous-phase aerosol at RH > 55% [*Galloway et al.*, 2008].

[12] HR-ToF-AMS elemental analysis [*Aiken et al.*, 2007, 2008] of aerosol produced from an aqueous solution containing 8.8 mM glyoxal and 16.8 mM methylamine reveals that the aerosol had a significantly lower N/C atomic ratio (0.32) than the starting mixture (0.49, calculated). Since molecules containing equal numbers of glyoxal and methylamine subunits (imine oligomers) are expected to have N/C ratios nearly identical (0.33) to those measured, the observed ratio is consistent with the formation of such oligomer products and the evaporation of excess methylamine. Thus, these experiments demonstrate that glyoxal can trap volatile amine compounds in the aerosol phase by oligomer-forming reactions that occur during cloud droplet evaporation. Aqueous-phase reactions between glyoxal and amines provide an explanation for the consistent co-detection of oligomers, amines and oxalic acid in Riverside, CA [*Denkenberger et al.*, 2007]. While a fraction of aqueous-phase glyoxal may be oxidized to oxalic acid during the ~15 min. lifetime of a cloud or fog droplet, the remaining glyoxal may oligomerize with amines upon droplet evaporation, producing aerosol containing oligomers, amines, and oxalic acid.

[13] While we have not measured reaction rates in this study, we have previously showed that glyoxal + amino acid reactions are fast enough to occur during and after cloud droplet evaporation under atmospheric conditions [*De Haan et al.*, 2009]. The atmospheric significance of glyoxal + methylamine reactions will therefore likely depend on the relative concentrations of glyoxal and amines in clouds and aerosol. Alkyl amines are produced by marine organisms, animal husbandry, biomass and fossil fuel burning, meat cooking, and industrial activities [*Murphy et al.*, 2007]. High (0.01–6 μg/m^3) levels of amine compounds have been measured in aerosol and fog in California's Central Valley [*Sorooshian et al.*, 2008; *Zhang and Anastasio*, 2001, 2003] and in winter aerosol in Logan, UT [*Silva et al.*, 2008]. Methylamine concentrations averaged 9 μM in Central Valley fog [*Zhang and Anastasio*, 2003]. Glyoxal concentrations in rural fog are typically lower [*Matsumoto et al.*, 2005; *Munger et al.*, 1995]. Functional group analysis of filtered particles collected at a range of sites indicates that amine groups typically account for 2–13% of organic matter and appear to correlate with fossil fuel burning [*Liu et al.*, 2009; *Russell et al.*, 2009]. This is roughly consistent with aerosol atomic N/C ratios detected by HR-ToF-AMS of ~0.02 in urban areas [*Aiken et al.*, 2008]. It is likely that the highest coincident levels of glyoxal and alkyl amines will be in polluted regions, in biomass burning plumes, and over biologically active agricultural and marine regions.

[14] If we assume that amine concentrations typically exceed those of glyoxal in clouds and aerosol, then we can use recent estimates of SOA formation from glyoxal [*Fu et al.*, 2008] to calculate an upper limit for the contribution of amines to global SOA budgets via reactions with glyoxal, using methylamine as a proxy since it is a dominant amine in cloudwater. 2.6 Tg C yr^{-1} SOA is formed globally by glyoxal if its uptake is irreversible [*Fu et al.*, 2008], which equals 7.6 Tg SOA yr^{-1} if glyoxal reacts with itself. Using our observation that the addition of equimolar quantities of methylamine to glyoxal solutions increased aerosol volumes by 48%, and assuming no change in aerosol density, a total of 11.2 Tg SOA yr^{-1} would be formed when glyoxal reacts with amines instead of itself, of which the increase of 3.6 Tg SOA yr^{-1} can be attributed to amines. This corresponds to an additional SOA source from methylamine of 1.4 Tg C yr^{-1} and 1.6 Tg N yr^{-1}, or about 3% of total WSOC [*Fu et al.*, 2009], a level that is consistent with aerosol amine measurements [*Liu et al.*, 2009; *Russell et al.*, 2009].

[15] **Acknowledgment.** This material is based upon work supported by the National Science Foundation under grant ATM-0749145.

References

Aiken, A. C., et al. (2007), Elemental analysis of organic species with electron ionization high-resolution mass spectrometry, *Anal. Chem.*, *79*, 8350–8358.

Aiken, A. C., et al. (2008), O/C and OM/OC ratios of primary, secondary, and ambient organic aerosols with high-resolution time-of-flight aerosol mass spectrometry, *Environ. Sci. Technol.*, *42*(12), 4478–4485, doi:10.1021/es703009q.

Baltensperger, U., et al. (2005), Secondary organic aerosols from anthropogenic and biogenic precursors, *Faraday Discuss.*, *130*, 265–278.

Canagaratna, M. R., et al. (2007), Chemical and microphysical characterization of ambient aerosols with the Aerodyne aerosol mass spectrometer, *Mass Spectrom. Rev.*, *26*(2), 185–222.

Carlton, A. G., et al. (2007), Atmospheric oxalic acid and SOA production from glyoxal: Results of aqueous photooxidation experiments, *Atmos. Environ.*, *41*, 7588–7602, doi:10.1016/j.atmosenv.2007.05.035.

De Haan, D. O., et al. (2009), Atmospheric condensed-phase reactions of glyoxal with amino acids, *Environ. Sci. Technol.*, *43*(8), 2818–2824, doi:10.1021/es803534f.

DeCarlo, P. F., et al. (2006), Field-deployable, high-resolution, time-of-flight aerosol mass spectrometer, *Anal. Chem.*, *78*, 8281–8289.

Decesari, S., et al. (2005), The water-soluble organic component of size-segregated aerosol, cloud water and wet depositions from Jeju Island during ACE-Asia, *Atmos. Environ.*, *39*, 211–222.

Denkenberger, K. A., et al. (2007), Real-time, single-particle measurements of oligomers in aged ambient aerosol particles, *Environ. Sci. Technol.*, *41*(15), 5439–5446, doi:10.1021/es070329I.

Fu, T.-M., D. J. Jacob, F. Wittrock, J. P. Burrows, M. Vrekoussis, and D. K. Henze (2008), Global budgets of atmospheric glyoxal and methylglyoxal, and implications for formation of secondary organic aerosols, *J. Geophys. Res.*, *113*, D15303, doi:10.1029/2007JD009505.

Fu, T.-M., et al. (2009), Aqueous-phase reactive uptake of dicarbonyls as a source of organic aerosol over eastern North America, *Atmos. Environ.*, *43*, 1814–1822, doi:10.1016/j.atmosenv.2008.12.029.

Galloway, M. M., et al. (2008), Glyoxal uptake on ammonium sulphate seed aerosol: Reaction products and reversibility of uptake under dark and irradiated conditions, *Atmos. Chem. Phys. Discuss.*, *8*, 20,799–20,838.

Hastings, W. P., et al. (2005), Secondary organic aerosol formation by glyoxal hydration and oligomer formation: Humidity effects and equilibrium shifts during analysis, *Environ. Sci. Technol.*, *39*(22), 8728–8735.

Igawa, M., et al. (1989), Analysis of aldehydes in cloud- and fogwater samples by HPLC with a postcolumn reaction detector, *Environ. Sci. Technol.*, *23*(5), 556–561.

Kalberer, M., et al. (2004), Identification of polymers as major components of atmospheric organic aerosols, *Science*, *303*, 1659–1662.

Kalberer, M., et al. (2006), Molecular size evolution of oligomers in organic aerosols collected in urban atmospheres and generated in a smog chamber, *Environ. Sci. Technol.*, *40*(19), 5917–5922, doi:10.1021/es0525760.

Liu, S., et al. (2009), Oxygenated organic functional groups and their sources in single and submicron organic particles in MILAGRO 2006 campaign, *Atmos. Chem. Phys. Discuss.*, *9*, 4567–4607.

Loeffler, K. W., et al. (2006), Oligomer formation in evaporating aqueous glyoxal and methyl glyoxal solutions, *Environ. Sci. Technol.*, *40*(20), 6318–6323.

Malloy, Q. G. J., et al. (2008), Secondary organic aerosol formation from primary aliphatic amines with NO_3 radical, *Atmos. Chem. Phys. Discuss.*, *8*, 12,695–12,720.

Matsumoto, K., et al. (2005), Dominant factors controlling concentrations of aldehydes in rain, fog, dew water, and in the gas phase, *Atmos. Environ.*, *39*, 7321–7329.

Munger, J. W., D. J. Jacob, B. C. Daube, L. W. Horowitz, W. C. Keene, and B. G. Heikes (1995), Formaldehyde, glyoxal, and methylglyoxal in air and cloudwater at a rural mountain site in central Virginia, *J. Geophys. Res.*, *100*, 9325–9333.

Murphy, S. M., et al. (2007), Secondary aerosol formation from atmospheric reactions of aliphatic amines, *Atmos. Chem. Phys.*, *7*, 2313–2337.

Nozière, B., P. Dziedzic, and A. Córdova (2007), Formation of secondary light-absorbing "fulvic-like" oligomers: A common process in aqueous and ionic atmospheric particles?, *Geophys. Res. Lett.*, *34*, L21812, doi:10.1029/2007GL031300.

Nozière, B., et al. (2009), Products and kinetics of the liquid-phase reaction of glyoxal catalyzed by ammonium ions (NH_4^+), *J. Phys. Chem. A*, *113*(1), 231–237, doi:10.1021/jp8078293.

Russell, L. M., S. Takahama, S. Liu, L. N. Hawkins, D. S. Covert, P. K. Quinn, and T. S. Bates (2009), Oxygenated fraction and mass of organic aerosol from direct emission and atmospheric processing measured on the R/VRonald Brown during TEXAQS/GoMACCS 2006, *J. Geophys. Res.*, *114*, D00F05, doi:10.1029/2008JD011275.

Silva, P. J., et al. (2008), Trimethylamine as precursor to secondary organic aerosol formation via nitrate radical reaction in the atmosphere, *Environ. Sci. Technol.*, *42*(13), 4689–4696, doi:10.1021/es703016v.

Sorooshian, A., et al. (2008), Comprehensive airborne characterization of aerosol from a major bovine source, *Atmos. Chem. Phys.*, *8*, 5489–5520.

Tolocka, M. P., et al. (2004), Formation of oligomers in secondary organic aerosol, *Environ. Sci. Technol.*, *38*(5), 1428–1434.

Zhang, Q., and C. Anastasio (2001), Chemistry of fog waters in California's Central Valley—Part 3: Concentrations and speciation of organic and inorganic nitrogen, *Atmos. Environ.*, *35*, 5629–5643.

Zhang, Q., and C. Anastasio (2003), Free and combined amino compounds in atmospheric fine particles ($PM_{2.5}$) and fog waters from northern California, *Atmos. Environ.*, *37*, 2247–2258.

D. O. De Haan, Department of Chemistry and Biochemistry, University of San Diego, 5998 Alcala Park, San Diego, CA 92110, USA. (ddehaan@sandiego.edu)

J. L. Jimenez and M. A. Tolbert, Department of Chemistry and Biochemistry, UCB 216, University of Colorado, Boulder, CO 80309-0216, USA.